ELSEVIER

Carbohydrate Polymers 49 (2002) 131–137

Carbohydrate Polymers

www.elsevier.com/locate/carbpol

Dissolution kinetics of guar gum powders. I. Methods for commercial polydisperse samples

Q. Wang[a,b], P.R. Ellis[a,*], S.B. Ross-Murphy[a]

[a]*Biopolymers Group, Division of Life Science, King's College London, Franklin-Wilkins Building, 150 Stamford Street, London SE1 9NN, UK*
[b]*Food Research Program, AAFC, 93 Stone Road West, Guelph, Ont., Canada N1G 5C9*

Received 6 February 2001; revised 9 July 2001; accepted 16 July 2001

Abstract

The ability to form molecular solutions, usually referred to as hydration or dissolution, is one of the most important properties of water-soluble polysaccharides and closely relates to their functionality in a plethora of biological and technological processes. The purpose of this study was to investigate the hydration kinetics of four commercially produced guar gum powders using viscosity development as an index of hydration rate. The following three empirical hydration models: (1) first-order kinetics; (2) logarithmic; and (3) the Weibull function, were evaluated for fitting to the hydration rate data of guar gum powders. Of the three models tested, the simple logarithmic function was found to be the most suitable for describing the behaviour of guar gum flours with satisfactory accuracy. By using this model the hydration process can be described by two hydration constants, which can be estimated from a linear plot. However, the hydration rate profile obtained from one guar gum sample of larger particle did not successfully fit any of the above models, producing instead a sigmoidal relationship that was more amenable to a polynomial function.

Keywords: Guar gum; Hydration; Dissolution

1. Introduction

1.1. Background

The hydration property of guar gum and other water-soluble non-starch polysaccharides (s-NSP) is an important characteristic in many applications where solutions of these polymers often need to be prepared. Thus, for example, in the pharmaceutical industry, s-NSP are used in drug delivery systems for increasing the transit time of novel dosage forms in the small intestine and for controlled release forms. The bioavailability of the drugs largely depends on the performance of the carrier system, which is closely related to the hydration behaviour of s-NSP. In addition, it has been found that s-NSP, including guar gum, can significantly modify metabolism and gut function of experimental animals and humans (Ellis, Rayment & Wang, 1996). For example, it is well-known that glucose drinks and starch-rich meals supplemented with guar gum attenuate the rise in postprandial blood glucose in healthy and diabetic subjects (Ellis, Apling, Leeds & Bolster, 1981; Ellis, Dawoud & Morris, 1991; Jarjis, Blackburn, Redfern & Read, 1984; Jenkins, Goff, Leeds, Alberti, Wolever, Gassull et al., 1976; Morgan, Tredger, Wright & Marks, 1990; O'Connor, Tredger & Morgan, 1981). This postprandial effect is probably, to a large extent, determined by the capacity of guar gum to hydrate and increase the viscosity of digesta in the upper gastrointestinal tract, causing a reduction in the rate of absorption of glucose (Ellis et al., 1996). Thus, the rate and degree of hydration of guar gum and other such polymers in determining their biological activity is of critical importance (Ellis & Morris, 1991; O'Connor et al., 1981). A range of physico-chemical properties of s-NSP and conditions in the gut environment inevitably influence the hydration properties of these polymers. Studies of the effects of such factors on the dissolution process are obviously fundamental to understanding the physiological mechanisms and optimising the clinical efficacy of s-NSP. These studies are also important in investigating the functional properties of s-NSP in general; e.g. viscosity-enhancing effects in the design of structured food products.

Knowledge about the hydration process of macromolecules is still somewhat limited, however. Although a number of theories and mathematical models have been developed, most of them still have various limitations for practical use (Abdou, 1989; Devotta, Ambeskar, Mandhare

* Corresponding author. Tel.: +44-20-7848-4238; fax: +44-20-7848-4082.
E-mail address: p.ellis@kcl.ac.uk (P.R. Ellis).

0144-8617/02/$ - see front matter
PII: S0144-8617(01)00327-7

& Mashelkar, 1994; Langenbucher, 1974; Ranade & Mashelkar, 1995). There are also models for the dissolution of polymers, which take into account the different macromolecular processes involved, including the reptation of polymer chains. (Brochard & de Gennes, 1983; Herman & Edwards, 1990; Narasimhan & Peppas, 1996; Peppas, Wu & von Meerwall, 1994). However, the polydispersity in particle size and molecular weight of particulate systems such as polysaccharide powders makes it extremely difficult to establish a theoretical model. Therefore, the development of semi-empirical models to describe the processes involved in the dissolution of polydisperse polymer systems is useful for practical purposes. The recent paper by Kravtchenko, Renoir, Parker and Brigand (1999) is another attempt to achieve this, but we feel our approaches, to be described in this and subsequent papers, are complementary to their model.

The current paper is therefore the first of three papers. It includes the development of a method for measuring hydration rate of polysaccharide powders and the selection of a suitable empirical model for further study of the hydration kinetics of these materials. Three types of models were selected and described as follows:

1.2. First order kinetics

A first order kinetics model is considered to be useful for describing physical and chemical reactions, including the hydration process. To, Mitchell, Hill, Bardon and Matthews (1994) used the following first order kinetics model to describe the hydration process of polysaccharide powders:

$$\ln\left(1 - \frac{\eta_t}{\eta_\infty}\right) = f(\eta) = -kt \tag{1}$$

where η_t is the viscosity of the dispersion at time t, η_∞ is the 'ultimate' viscosity and k is the time constant related to the rate of viscosity development. This implies that the plots of either $f(\eta)$ or $g(\eta)$ (see Eq. (2)) vs. time t, are straight lines.

Eq. (1) uses a first power law for the viscosity dependence on concentration, which is approximately true for the data collected below C^*, i.e. when $\eta \propto C^1$. However, in our experiment with guar gum powders, the concentration of dissolved polymer was found to be higher than C^* within the first 1–3 min of the hydration process. An appropriate modification in this case is to replace C^1 by a $C^{3.5}$ power law, for the viscosity dependence on concentration according to previous workers (for example, Lapasin & Pricl, 1995; Robinson, Ross-Murphy & Morris, 1982), which is therefore written as:

$$\ln\left(1 - \left(\frac{\eta_t}{\eta_\infty}\right)^{1/3.5}\right) = g(\eta) = -kt \tag{2}$$

As will be discussed later, neither model (Eqs. (1) and (2)) fits our data well.

In succeeding sections we will derive alternative models for the same hydration kinetics results. We comment here that for formal studies of *chemical* kinetics then concentrations (or, more formally, the activities) of the dissolved species are required. However, when we are concerned with *hydration* kinetics, it may be more appropriate to consider the viscosity results directly. As we see below, this is because there may not be a simple two-way mapping between viscosity and concentration, for systems that are still only partly hydrated.

1.3. Logarithmic model

Preliminary experiments of the hydration of the guar gum flours tested in the current study, indicated that a plot of $\ln(1 - \eta_t/\eta_\infty)$ vs. time t was similar in shape to the logarithmic function $y = \log_a t$, when $0 < a < 1$, $y = \ln(1 - \eta_t/\eta_\infty)$. The curve of $y = \log_a t$ passes through the point (1,0). If we make the transformation $t' = t - 1$, then the curve of $y = \log_a t'$ will pass through the origin (0,0), and, as seen in Section 3, is similar in shape to our hydration curves. In order to be consistent with the form of $\ln(1 - \eta_t/\eta_\infty)$, and since $\log_a t = \ln t/\ln a$, the following natural logarithm function was selected initially to fit the hydration data:

$$\ln\left(1 - \frac{\eta_t}{\eta_\infty}\right) = k\ln[a(t + t_0)] \tag{3}$$

1.4. Weibull function

The Weibull function is a statistical distribution function originally proposed by Weibull (1951), who found it to be applicable to a wide field of problems. A number of examples include size distribution of fly ash, yield strength of a bofors steel and the possibility of failure in a chain consisting of several links. If X represents the individuals of a population in question, the distribution function of X, $F(x)$, may be defined as the number of all individuals having $X \leq x$, divided by the total number of individuals. According to Weibull, any distribution function may be written in the form of:

$$F(x) = 1 - \mathrm{e}^{-\varphi(x)} \tag{4}$$

where $\varphi(x)$ is a function that only has to satisfy the general condition of being a positive, non-decreasing function and vanishing at a value Ω. One of the simple functions satisfying this condition is $[(x - \Omega)/\alpha]^\beta$.

Thus, we have the general distribution function (Weibull function):

$$F(x) = 1 - \mathrm{e}^{-[(x-\Omega)/\alpha]^\beta} \tag{5}$$

To apply this function to the hydration problem, the distribution function $F(x)$ was conventionally chosen as, $F(t) = 1 - \eta_t/\eta_\infty$, the fraction remaining undissolved at time t. Thus, Ω, α and β are the parameters that relate to viscosity development during the hydration process.

2. Experimental

2.1. Materials and characterisation methods

Guar gum flours of different molecular weight and particle size were used in this study. These included commercial food grades M150, M90 (Meyprogat range; Meyhall Chemical AG, Rhodia Food, Kreuzlingen, Switzerland), RG30 (Hercules, London, UK) and a laboratory-prepared sample named Master g (Meyhall Chemical AG). For characterisation of these samples, all measurements of particle size, galactomannan content and intrinsic viscosity were performed in duplicate or triplicate.

Particle sizes of the samples were measured using a Malvern 2600 Laser Diffraction Sizer (Malvern Instruments Ltd, Worcs, UK). A monochromatic beam of light was produced by a low-power visible laser (wavelength = 633 *nm*) passing through a lens system of focal length 100 mm. Approximately 0.5 g of each sample was sonicated in 10 ml butan-1-ol for 10 min to disperse the sample evenly. Approximately 2–5 drops of the sample mixture were dropped into the light scattering cell filled with butan-1-ol so that obscuration values fell in the range 0.15–0.2. Malvern's own non-linear least squares analysis was used to calculate the mean particle size.

The galactomannan content and the galactose/mannose ratio of the guar gum samples were determined by gas–liquid chromatography following acid hydrolysis and derivitisation of the carbohydrates to alditol acetates (Englyst, Quigley, Hudson, & Cummings, 1992). This method was slightly modified by hydrating the samples overnight in phosphate buffer, as opposed to 40 min suggested by Englyst et al. (1992), to allow more complete hydration of the galactomannan fraction (Rayment, Ross-Murphy & Ellis, 1995).

Viscosity measurements for determining intrinsic viscosity were performed in a dilution capillary viscometer (Cannon Ubbelohde Dilution B glass viscometer, size 50, 0.8–4.0 cSt; Glass Artifact (Viscometers), UK) suspended in a constant water bath at 25°C. Intrinsic viscosity was determined by double extrapolation of the Huggins and Kramer equations (i.e. extrapolation of η_{sp}/C and $\ln \eta_r/C$ plots to zero C, where η_{sp} is the specific viscosity and η_r is the viscosity of polysaccharide relative to water) (Robinson et al., 1982).

Some of the information on the physical and chemical characteristics of the samples is listed in Table 1.

Table 1
Moisture content (MC), galactomannan content (GM) as % dry matter, ratios of galactose to mannose (Gal/Man), intrinsic viscosity [η] and mean particle size (d_m) of guar gum powders. Values are means of duplicates or triplicates (N.D.: not determined, SD: standard deviation)

Samples	Master g	M150	RG30	M90
MC (%)	10.5	12.8	11.1	8.6
GM (%) ± SD	85.3 ± 4.7	87.8 ± 4.8	88.3	91.3 ± 2.5
Gal/Man	0.67	0.68	0.65	0.70
[η] (dl/g) ± SD	17.3 ± 0.3	17.5 ± 0.2	14.5 ± 0.2	10.5 ± 0.2
d_m (μm) ± SD	81 ± 6	60.7 ± 1.5	N.D.	70.8 ± 3.7

2.2. Hydration method

The hydration method used in this study is a modified technique previously developed for measuring the hydration rate of pharmaceutical preparations of guar gum (Ellis & Morris, 1991). Hydration was performed in a mixing box constructed in the King's College workshop and fitted inside an incubator to allow good control of experimental temperature. A 1% (w/w) dispersion of guar gum in distilled water (total volume 500 ml) was prepared and sealed in a screw-top glass jar (diameter 84 mm, volume 675 ml), which was then rotated end-over-end at a pre-set speed during the hydration process. The 'rotating radius' of the centre of the sample jar is 65 mm.

The procedure involved carefully sprinkling the guar gum powder into a rapidly swirling vortex of distilled water in a glass jar. A magnetic stirrer was used to create the vortex in the distilled water. Samples was placed in a sieve (355 μm aperture, 40 mesh) with a sealed centre, so that by manually tapping the sieve, the samples could be dispersed through the ring-shaped sieve area (Fig. 1). This encouraged a rapid and even dispersion of the sample into the wall of the water vortex created by the magnetic stirrer, thus minimising aggregation of particles and producing a homogeneous polymer solution. The time taken to add the whole of each sample to the water was controlled within 60–90 s. The start of hydration was taken as the moment the guar gum made contact with water.

The glass jars were then immediately sealed and rotated end-over-end in the mixing box at a speed of 6 rpm (or 10 rpm, for Master g), the estimated minimum speed needed to promote dispersion and hydration of guar gum. The dissolution process was monitored by the measurement of viscosity development at 25°C. The viscosity was measured every 10 min in the first hour and thereafter every 30 min until 5 h. An additional measurement was taken following thorough homogenising with an Ultra-Turrax mixer. This measurement is referred to as the 'ultimate' viscosity, the point at which it was considered that the samples had been

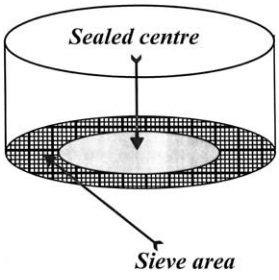

Fig. 1. The sieve used for dispersing guar gum samples into the water vortex in the screw-top glass jars. The centre of the sieve was sealed so that the samples can only be dispersed through the ring shaped sieve area.

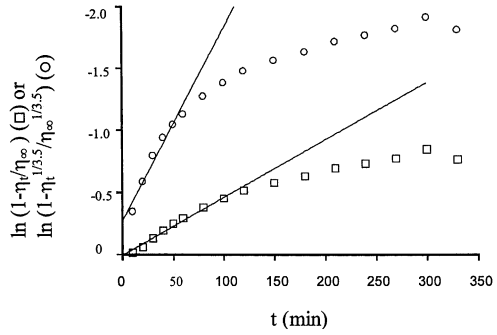

Fig. 2. Examples of hydration data of guar gum sample (Master g) fitted to a first order kinetics model according to Eqs. (1) and (2).

completely hydrated. An aliquot of approximately 2 ml was taken from the batch solution at each time. The measurement of viscosity was affected by the inclusion of the undissolved particles. At present it is difficult to evaluate the contribution of these particles to the viscosity of the dispersion, because of the lack of information on factors such as the volume fraction, and the size and shape of the particles (Rayment, Ross-Murphy & Ellis, 2000). Indeed all of these factors are changing continuously during the hydration process. Thus, before viscosity measurements were made aliquots of the guar gum solution were centrifuged on a microcentrifuge (Eppendorf 5414S, 15,000 rpm) for 60–90 s. These supernatants were used for the measurements of viscosity development during the hydration process.

Viscosity measurements were performed on either a Brookfield RVT viscometer, using spindle 4 at 20 rpm (average shear rate $\sim 4.1\ s^{-1}$), or a Rheometrics Fluid Spectrometer (RFSII), using plate–plate configurations (50 mm in diameter and 1 mm gap). In the latter case, zero-shear viscosity, η_0, was estimated from the mean value of the first four experimental points at the lowest shear rate, corresponding to the Newtonian plateau. 1% w/w solutions were prepared on the basis of dry matter content of the materials (not on the amount of galactomannan). Each experiment was performed on four different occasions and the mean of these four replicates was used in subsequent data analysis.

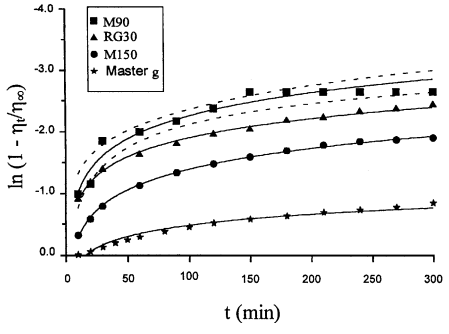

Fig. 3. Hydration data of different guar gum flours fitted by Eq. (3). Dotted lines indicate 95% confidence intervals. Viscosity of Master g was measured using the RFSII; the rest of the data was obtained from the Brookfield RVT viscometer.

Table 2
Summaries of curve fitting results of hydration kinetics of different guar gum samples using the logarithmic model (Eq. (3)). s^2 is the estimation of variance (sum of squares/degrees of freedom)

Samples	Parameters				
	a	K	B	r^2	s^2
Master g	0.063	−0.261	0.721	0.962	3×10^{-3}
M150	0.176	−0.485	0.841	0.998	6×10^{-4}
RG30	0.704	−0.446	0.157	0.996	1×10^{-3}
M90	0.657	−0.538	0.289	0.952	2×10^{-2}

3. Results

3.1. First order kinetics model

In all the guar gum samples tested, it was found that the first order kinetics model according to Eqs. (1) and (2) did not fit the hydration data closely. We would not expect that to be true for the first of these, because all the data are close to, or above C^*, even for the initial (10 min) time reading. One set of hydration data for Master g is shown in Fig. 2. In both plots for this sample the experimental data points deviated from the initial linear region at about 120 and 60 min, respectively. At these times the dispersions developed only about 40 and 25% of their ultimate viscosity, respectively. Recently, Kravtchenko et al. (1999) reported that the dissolution process of pectin powder could only be described by simple first order kinetics under so-called 'dispersing conditions'; thus to compensate they introduced a sum of two exponential terms. In their work, such conditions were achieved by mixing pectin powder with ground sucrose to prevent lump formation during dissolution. They also demonstrated that under non-dispersing conditions, the dissolution of pectin powder could be better described by the summed exponential function.

3.2. Logarithmic model

The results of the data fitting for samples of M150, M90, RG30 and Master g using a logarithmic model (Eq. (3)) are illustrated in Fig. 3. The statistics of the results (Table 2) showed that the present model fitted the experimental data reasonably well, as indicated by the high correlation coefficients ($r^2 > 0.95$) and small s^2, the latter being an estimate of variance (s^2 is the sum of squares/degrees of freedom).

During the curve fitting process, t_0 was found not to differ statistically from zero ($p \leq 0.1$) for any of the four samples used. This implies that the transformation $t' = t - 1$ for the logarithmic function, $y = \log_a t'$, was not necessary. This is probably because that there was a short time lag before the dissolution process starts, corresponding to the initial stage of swelling of the particles. The time lag was more pronounced for samples of large particle size, as will be show in subsequent papers. It is reasonable to assume

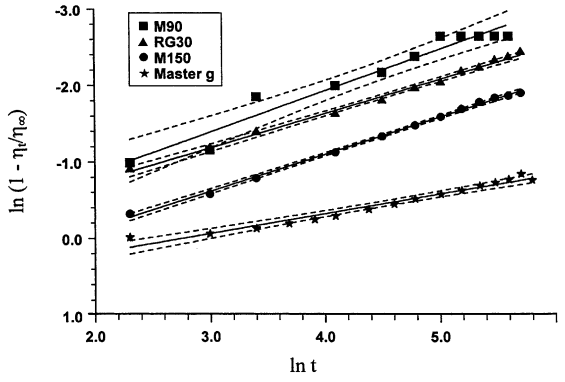

Fig. 4. The same hydration data as seen in Fig. 3, but fitted to Eq. (7). Dotted lines indicate 95% confidence intervals.

therefore that $t_0 = 0$, and, accordingly, Eq. (3) can be simplified as:

$$\ln\left(1 - \frac{\eta_t}{\eta_\infty}\right) = k\ln[at] \tag{6}$$

which expands to:

$$\ln\left(1 - \frac{\eta_t}{\eta_\infty}\right) = b + k\ln t \tag{7}$$

where $b = k \ln a$. Eq. (7) implies that the plots of $\ln(1 - \eta_t/\eta_\infty)$ vs. $\ln t$ should be a series of straight lines, each with a slope k and intercept b.

Fig. 4, which corresponds to the data in Fig. 3, shows clearly that three of the four samples (M150, M90 and RG 30) gave straight lines with excellent linearity. The curve fitting results were the same as those in Table 2. For M90, a slightly poorer correlation was obtained using the present model to fit the experimental data. Nevertheless, as indicated by the 95% confidence intervals in Fig. 4, the linear relationship was still valid ($r^2 = 0.95$). The poorer correlation is attributed to the quality of experimental data itself, indicated by the relatively high value of s^2 (0.02), rather

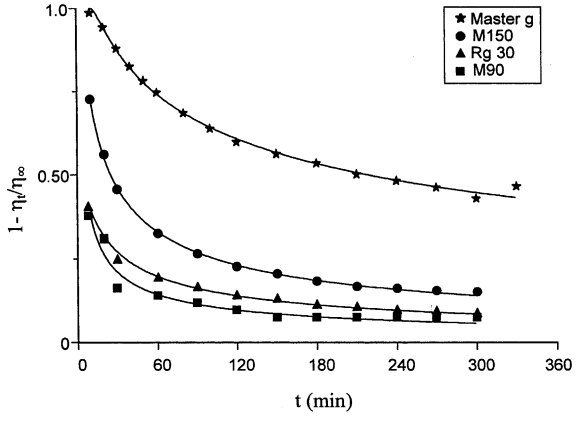

Fig. 5. Examples of the Weibull function fitted with hydration data obtained from guar gum flours. Data of Master g was obtained by using RFSII; the rest of the data by the Brookfield viscometer.

Table 3
Summaries of curve fitting results of hydration kinetics of guar gum samples using the Weibull function (Eq. (5)). s^2 is the estimation of variance (sum of squares/degrees of freedom)

Samples	Parameters				
	Ω	α	β	r^2	s^2
Master g	10	95	−0.47	0.996	1×10^{-4}
M150	1.9	12.6	−0.60	0.998	3×10^{-4}
RG30	−6.6	5.3	−0.63	0.994	7×10^{-5}
M90	1	2.6	−0.61	0.946	6×10^{-4}

than the suitability of the model. In any case, the relatively low viscosity of 1% w/v M90 solution made it difficult to detect the smaller changes at each time point. However, this could be improved by using a more sensitive geometry, such as the Couette system on the RFS II.

3.3. Weibull function

The hydration data of different guar gum samples were found to fit the Weibull function very well regardless of the difference in molecular weight, particle size and types of guar gum samples used (Fig. 5). The fitted parameters are tabulated in Table 3. From Fig. 5 and Table 3 it can be seen that parameter β was a shape factor for the hydration curve. Thus, the hydration curves of sample M150, M90 and RG30 were similar in shape and their β values were approximately the same (−0.6). A smaller absolute value of β (−0.47) and significantly slower hydration rate was obtained for Master g, which had the largest particle size.

The second parameter α defines the time scale for the dissolution process, since the larger the α value the slower the hydration rate. Therefore, α can be used to compare the hydration rate with samples that have similar β values. For samples M150, RG30 and M90, which have similar β values, it is clear that the hydration rate increased while α decreased. The third parameter Ω, is related to the apparent induction time of dissolution controlled by the initial swelling time of the polymers. Dissolution starts only when $(t - \Omega) > 0$.

4. Discussions

The first point to clarify, is why we adopt the procedure of fitting the viscosity directly, rather than the concentration of dissolved material. This would be more appropriate from the viewpoint of conventional chemical kinetics, but even though we centrifuged the extracted samples to remove totally undissolved ('filler' phase material) we still do not have an equilibrium system. In other words, the viscosity even after filtration has a complex contribution from molecularly dissolved polymer, supramolecular but essentially hydrated material and solvent, so the relationship between the measured viscosity at any time ($<\infty$) is not necessarily a direct one. Consequently, the idea that we use the ultimate

Table 4
Hydration index $t_{0.8}$ calculated from Weibull function (model 1) and the logarithmic model (model 2)

	Model 1	Model 2
Samples	$t_{0.8}$ (min)	$t_{0.8}$ (min)
Master g	2320	7647
M150	155	156
RG30	50	52
M90	31	30

viscosity vs. concentration plots to back calculate the concentration of molecularly dispersed material is one we dismissed fairly early on. We were not convinced there was, at any particular shear rate, a one-to-one mapping between concentration and the measured viscosity *of the still hydrating system*.

4.1. Alternative models for hydration kinetics

Conventionally, $t_{0.5}$, the half-life of a reaction, is used to describe the duration of a reaction. Similarly, we can define a hydration index, $t_{0.8}$, the time needed for viscosity of the dispersion to reach 80% of the ultimate viscosity. The reason for choosing this time period, rather than $t_{0.5}$, was that it covered the main period of hydration process during which most of the viscosity had developed and also that the viscosity was approaching the plateau value, or ultimate viscosity. However, when other fractional time periods were selected, for example, $t_{0.5}$ or $t_{0.9}$, a similar profile was obtained. Thus, the logarithmic model (Eq. (7)) can be rearranged as:

$$\ln\left\{\left(1 - \frac{\eta_t}{\eta_\infty}\right)/t^k\right\} = b \tag{8}$$

thus,

$$t = \left\{\left(1 - \frac{\eta_t}{\eta_\infty}\right)/e^b\right\}^{1/k} \tag{9}$$

substituting $\eta_{0.8} = 0.8\eta_\infty$ in the above equation gives:

$$t_{0.8} = \left\{\frac{0.2}{e^b}\right\}^{1/k} \tag{10}$$

When $\eta_{0.8} = 0.8\eta_\infty$ and $f(t) = 1 - \eta_t/\eta_\infty$ are substituted into the Weibull function (Eq. (5)), the hydration index, $t_{0.8}$, is given as:

$$t_{0.8} = \alpha\{\ln(0.8)\}^{1/\beta} + \Omega \tag{11}$$

The use of the hydration index $t_{0.8}$ enabled us to compare the results predicted from the logarithmic model and the Weibull function, both of which fitted our hydration data successfully. Table 4 lists the hydration index $t_{0.8}$ for each of the four guar gum samples calculated from the Weibull function (model 1) and our logarithmic model (model 2). The indices obtained from these two models agreed very well for the three commercial guar gum flours. However, in contrast, the $t_{0.8}$ value for Master g, calculated from model 2, was significantly higher than that obtained from model 1. This is because that the logarithmic model was suitable only for samples have hydration curves with exponential growth in viscosity.

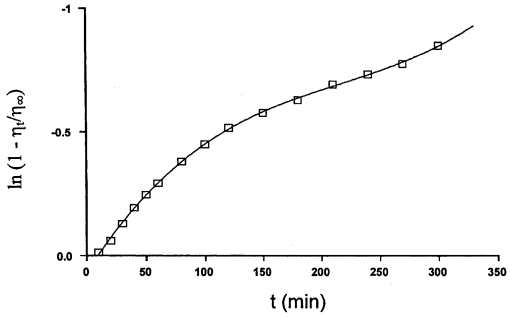

Fig. 6. Hydration curve of Master g fitted to a polynomial function showing the time lag in the first 15 min and the upturn after about 200 min. The solid line is the cubic regression of the data ($r^2 = 0.999$).

Further experiments (to be published) have shown that for some guar gum samples with larger particle size (and therefore lower hydration rate), the hydration curve was actually an exponential sigmoid curve. Indeed, the hydration curve of Master g did exhibit a small lag phase in the first ~15 min and a tendency to produce an upturn in the curvature at about 200 min when fitted by a polynomial model (Fig. 6). This increase in hydration rate after 200 min may be ascribed to the disintegration of large particles or lumps formed during the initial hydration stage. The difficulty of modelling the hydration data obtained from large particle size samples and the mechanism of their behaviour during dissolution will be dealt with in a subsequent paper.

For commercial guar gum flours, models 1 and 2 can be used to simulate the hydration process satisfactorily. However, the logarithmic model has the advantage that it is much easier to extract the hydration parameters from the linear transform of the model (Eq. (7)). In contrast, since the Weibull function has too many arbitrary parameters, the curve fitting process was found to be very laborious. The difficulties lie in the pre-determination of the parameter Ω at the beginning of the curve fitting process. The function was actually very sensitive to the pre-set Ω value. Although the Weibull function can also be transformed into a linear form, the curve fitting was arduous without the correct Ω values. Furthermore, it is difficult to explain why Ω can sometimes be negative, as in the case of the RG30 sample (see Table 3). Langenbucher (1972) used this model for some pharmaceutical tablets with the assumption that $\Omega = 0$. However, we found this relationship did not hold for guar gum powders.

5. Conclusions

Three hydration models were evaluated for the hydration process of guar gum powders. The Weibull function has been found to be useful for describing the hydration kinetics

of these polymers. However, the use of this model was limited because of the complexity of the curve fitting process. A simple logarithmic model was found to be more suitable for describing the common commercial guar gum flours with satisfactory accuracy. By using this model the hydration process can simply be described by two hydration constants, which can be obtained from a linear plot. It is anticipated that this model would be useful also for studying other high-molecular weight polymer powders, although further experiments would be needed to test this.

Acknowledgements

The authors gratefully acknowledge the financial support from Meyhall Chemical A.G. (Rhodia Food), Kreuzlingen, Switzerland and Mr W.C. Wielinga from the same company for preparing some of the guar gum samples. Mr V. Dawes, and Mr X.M. Zeng, of King's College London, U.K. are thanked for help and advice with the method for determining particle size. The Rheometrics instrument (RFSII) was purchased courtesy of BBSRC, under grant F01033.

References

Abdou, H. M. (1989). *Theory of dissolution*, *Dissolution, bioavailability and bioequivalence*. Easton, PA: Mack Publishing Company.

Brochard, F., & de Gennes, P. G. (1983). Kinetics of polymer dissolution. *Physicochemical Hydrodynamics*, *4*, 313–322.

Devotta, I., Ambeskar, V. D., Mandhare, A. B., & Mashelkar, R. A. (1994). Life time of a dissolving polymer particle. *Chemical Engineering Science*, *49*, 645–654.

Ellis, P. R., & Morris, E. R. (1991). Importance of the rate of hydration of pharmaceutical preparations of guar gum; a new in vitro monitoring method. *Diabetic Medicine*, *8*, 378–381.

Ellis, P. R., Apling, E. C., Leeds, A. R., & Bolster, N. R. (1981). Guar bread: acceptability and efficacy combined. Studies on blood glucose, serum insulin and satiety in normal subjects. *British Journal of Nutrition*, *46*, 267–276.

Ellis, P. R., Dawoud, F. M., & Morris, E. R. (1991). Blood glucose, plasma insulin and sensory responses to guar-containing wheat breads: effects of molecular weight and particle size of guar gum. *British Journal of Nutrition*, *66*, 363–379.

Ellis, P. R., Rayment, P., & Wang, Q. (1996). A physico-chemical perspective of plant polysaccharides in relation to glucose absorption, insulin secretion and the entero-insular axis. *Proceedings of Nutrition Society*, *55*, 881–898.

Englyst, H., Quigley, M. E., Hudson, G. J., & Cummings, J. H. (1992). Determination of dietary fibre as non-starch polysaccharides by gas–liquid chromatography. *Analyst*, *117*, 1707–1714.

Herman, M. F., & Edwards, S. F. (1990). A reptation model for polymer dissolution. *Macromolecules*, *23*, 3662–3671.

Jarjis, H. A., Blackburn, N. A., Redfern, J. S., & Read, N. W. (1984). The effect of isphagula (Fybogel and Metamucil) and guar gum on glucose tolerance in man. *British Journal of Nutrition*, *51*, 371–378.

Jenkins, D. J. A., Goff, D. V., Leeds, A. R., Alberti, K. G. M. M., Wolever, T. M. S., Gassull, M. A., & Hockaday, T. D. R. (1976). Unabsorbable carbohydrates and diabetes: decreased post-prandial hyperglycaemia. *The Lancet*, *2*, 172–174.

Kravtchenko, T. P., Renoir, J., Parker, A., & Brigand, G. A. (1999). A novel method for determining the dissolution kinetics of hydrocolloid powders. *Food Hydrocolloids*, *13*, 219–225.

Langenbucher, F. (1972). Linearization of dissolution rate curves by the Weibull distribution. *Journal of Pharmacy and Pharmacology*, *24* (12), 979–981.

Langenbucher, F. (1974). Material and method parameters in dissolution rate studies. *Pharmaceutica Acta Helvetiae*, *49* (5–6), 187–192.

Lapasin, R., & Pricl, S. (1995). *Rheology of industrial polysaccharides: theory and applications*, Glasgow, UK: Blackie Academic and Professional.

Morgan, L. M., Tredger, J. A., Wright, J., & Marks, V. (1990). The effect of soluble- and insoluble-fibre supplementation on post-prandial glucose tolerance, insulin and gastric inhibitory polypeptide secretion in healthy subjects. *British Journal of Nutrition*, *64*, 103–110.

Narasimhan, B., & Peppas, N. A. (1996). On the importance of chain reptation in models of dissolution of glassy polymers. *Macromolecules*, *29*, 3283–3291.

O'Connor, N., Tredger, J., & Morgan, L. (1981). Viscosity differences between various guar gums. *Diabetologia*, *20*, 612–615.

Peppas, N. A., Wu, J. C., & von Meerwall, E. D. (1994). Mathematical-modeling and experimental characterization of polymer dissolution. *Macromolecules*, *27*, 5626–5638.

Ranade, V. R., & Mashelkar, R. A. (1995). Convective diffusion from a dissolving polymeric particle. *American Institute of Chemical Engineers*, *41* (3), 666–676.

Rayment, P., Ross-Murphy, S. B., & Ellis, P. R. (1995). Rheological properties of guar galactomannan and rice starch mixtures. 1. Steady shear measurements. *Carbohydrate Polymers*, *28*, 121–130.

Rayment, P., Ross-Murphy, S. B., & Ellis, P. R. (2000). Effect of size and shape of particulate inclusions on the rheology of guar galactomannan solutions. *Carbohydrate Polymers*, *43* (1), 1–9.

Robinson, G., Ross-Murphy, S. B., & Morris, E. R. (1982). Viscosity–molecular weight relationships, intrinsic chain flexibility, and dynamic solution properties of guar galactomannan. *Carbohydrate Research*, *107*, 17–32.

To, K. -M., Mitchell, J. R., Hill, S. E., Bardon, L. A., & Matthews, P. (1994). Measurement of hydration of polysaccharides. *Food Hydrocolloids*, *8*, 243–249.

Weibull, W. (1951). A statistical distribution function of wide applicability. *Journal of Applied Mechanics*, *18*, 293–297.